Applying distance sampling to fin whale calls recorded by single seismic instruments in the northeast Atlantic

Danielle Harris[a)]
Centre for Research into Ecological and Environmental Modelling, The Observatory, Buchanan Gardens, University of St. Andrews, St. Andrews, Fife, KY16 9LZ, United Kingdom

Luis Matias
Instituto Dom Luiz, Universidade de Lisboa, Lisbon, Portugal 1749-016

Len Thomas
Centre for Research into Ecological and Environmental Modelling, The Observatory, Buchanan Gardens, University of St. Andrews, St. Andrews, Fife, KY16 9LZ, United Kingdom

John Harwood
Scottish Oceans Institute, Institiud Chuantan na h-Alba, East Sands, St Andrews, KY16 8LB, Scotland, United Kingdom

Wolfram H. Geissler
Alfred-Wegener-Institut für Polar- und Meeresforschung, Am Alten Hafen 26, D-27568 Bremerhaven, Germany

(Received 30 June 2012; revised 25 July 2013; accepted 12 August 2013)

Automated methods were developed to detect fin whale calls recorded by an array of ocean bottom seismometers (OBSs) deployed off the Portuguese coast between 2007 and 2008. Using recordings collected on a single day in January 2008, a standard seismological method for estimating earthquake location from single instruments, the three-component analysis, was used to estimate the relative azimuth, incidence angle, and horizontal range between each OBS and detected calls. A validation study using airgun shots, performed prior to the call analysis, indicated that the accuracy of the three-component analysis was satisfactory for this preliminary study. Point transect sampling using cue counts, a form of distance sampling, was then used to estimate the average probability of detecting a call via the array during the chosen day. This is a key step to estimating density or abundance of animals using passive acoustic data. The average probability of detection was estimated to be 0.313 (standard error: 0.033). However, fin whale density could not be estimated due to a lack of an appropriate estimate of cue (i.e., vocalization) rate. This study demonstrates the potential for using a sparse array of widely spaced, independently operating acoustic sensors, such as OBSs, for estimating cetacean density.
[http://dx.doi.org/10.1121/1.4821207]

PACS number(s): 43.30.Sf, 43.80.Ka [JJF] Pages: 3522–3535

I. INTRODUCTION

Monitoring marine mammals using passive acoustic instruments is an increasingly popular survey approach. Provided that the species of interest makes a sound that can be used as a cue to indicate that an individual is present, then passive acoustic monitoring can overcome some of the limitations of visual surveys. Acoustic surveys are less sensitive to weather conditions and can be conducted 24 h a day. In addition, acoustic monitoring equipment can be left *in situ* for extended time periods, enabling long term datasets to be collected throughout all seasons.

Passive acoustic studies have been used to address a variety of research issues, ranging from fine scale studies of animal behavior (e.g., lunge feeding behavior; Goldbogen *et al.*, 2013) to population level processes (e.g., migration patterns; Stafford *et al.*, 1999). Passive acoustic instruments can either be fixed to the seafloor or be mobile, e.g., hydrophones can be towed by a ship or attached to oceanographic vehicles such as seagliders (Moore *et al.*, 2008). Passive acoustic instruments may be deployed as part of a dedicated marine mammal survey (e.g., Kerosky *et al.*, 2012), or they may have another primary purpose but can be used for marine mammal monitoring. For example, cabled hydrophone arrays at the U.S. Navy's Atlantic Undersea Test and Evaluation Center (AUTEC) and the Pacific Missile Range Facility (PMRF) have been used in several cetacean studies (e.g., Marques *et al.*, 2009; Martin *et al.*, 2013).

In this study, fin whale (*Balaenoptera physalus*) calls were recorded by an array of ocean bottom seismometers (OBSs) deployed on the seafloor near the Straits of Gibraltar in the northeast Atlantic Ocean. Despite their low sampling rate (limiting their use to monitoring the low frequency calls of baleen whales) OBSs provide a useful source of opportunistic cetacean monitoring data. Data from OBSs have already

[a)]Author to whom correspondence should be addressed. Electronic mail: dh17@st-andrews.ac.uk

been used in several studies to track the movement of blue (*B. musculus*) and fin whales (e.g., Rebull *et al.*, 2006; Frank and Ferris, 2011; Wilcock, 2012; Soule and Wilcock, 2013)[1] to investigate habitat use (Wilcock and Thomson, 2010) and to investigate potential behavioral responses to both anthropogenic and natural sound sources (McDonald *et al.*, 1995; Dunn and Hernandez, 2009). In these studies, either azimuth was estimated using a single OBS or arrays of OBSs were used to provide locations of calling animals. Here we present a seismological method, the three-component method, which has been modified to estimate ranges to calling animals using a single OBS. Furthermore, we demonstrate how calls recorded on an array of such instruments can be analyzed using distance sampling (Buckland *et al.*, 2001), a popular wildlife abundance estimation method. Distance sampling allows the probability of detecting fin whale calls to be estimated; this is a key step to ultimately estimating fin whale density or abundance using acoustic data.

The paper is laid out as follows. We begin (Sec. II) by describing the three-component method for estimating range. We then (Sec. III) describe the study area and seismic array and (Sec. IV) a validation study of the three-component method, undertaken within this area using airgun shots produced by a seismic survey vessel where source location was known. We next (Sec. V) apply these methods to fin whale calls and demonstrate (Sec. VI) how the outputs can be used in a distance sampling analysis. We finish (Sec. VII) with a discussion of the limitations and potential of the approach.

II. THE THREE-COMPONENT METHOD

Earthquake location using a single station (e.g., a single OBS) is a well-known problem in seismology. Frohlich and Pulliam (1999) provide a review of single-station location methods and their effectiveness in earthquake source parameter estimation. All methods require that seismometers record three components of seismic movement (on two horizontally orientated geophones and one vertically orientated geophone), and they also need a good knowledge of the propagation velocities in the media, both for primary and secondary waves (hereafter referred to P- and S-waves). If the seismic event is close to the earth's surface or its focal depth is known, then the single-station methods provide a good estimate of the earthquake epicenter. In this work, a single-station method proposed by Roberts *et al.* (1989), known as the three-component analysis, is used to estimate the relative station-to-source azimuths and apparent emergence angles of signals produced in the water column. These parameters are then used to estimate incidence angles in the water column and horizontal ranges to the sources of the signals. A simplified overview of the method is given, followed by further details of some important considerations.

A. Single-station location method overview

Pressure waves generated in the water column (denoted P in Fig. 1) above an OBS (denoted S in Fig. 1) reach the seafloor with incidence angle (i) (Fig. 1). They are then converted to P- and SV-seismic waves that propagate into the sediments. SV-waves are S-waves where the ground vibration is vertical rather than horizontal (Doyle, 1995). The OBS measures the ground velocity caused by both P- and SV-waves. If the seismic signal (V_{seis}) is decomposed into its horizontal and vertical components (A_h and A_z) then the apparent emergence angle (i_{app}) of the ray traveling in the sediments can be estimated by the equation

$$i_{app} = \tan^{-1}\left(\frac{A_h}{A_z}\right). \quad (1)$$

Using both horizontal components of the ground velocity (A_x and A_y), the azimuth of the source (ϕ) can also be derived by the relationship

$$\phi = \tan^{-1}\left(\frac{A_x}{A_y}\right). \quad (2)$$

Here A_x, A_y, and A_z are the amplitudes of channels x, y, and z, respectively, and

$$A_h = \sqrt{{A_y}^2 + {A_x}^2}. \quad (3)$$

If the height of the source above the seafloor (h_w), the source azimuth (ϕ) and the wave incidence angle in the water layer (i) is known, then the horizontal range (r) and the coordinates of the source (a,b) can be computed by trigonometry, as follows (Fig. 1):

$$r = h_w \tan(i), \quad (4)$$

$$a = -r\sin(\phi), \quad (5)$$

$$b = -r\cos(\phi). \quad (6)$$

The range estimation presented here has been simplified from the analysis in Roberts *et al.* (1989) because a homogenous vertical sound speed profile is assumed in order to estimate r [Eq. (4)], i.e., a realistic propagation model is not considered. In addition, in this study the horizontal geophones are denoted x and y, as opposed to E and N (denoting eastern and northern bearings, respectively), because the true orientation of the seismometer was not known. The three-component method cannot estimate the absolute azimuth and location of an acoustic source unless the true orientation of the sensors is provided (the true orientation can be measured *in situ* by remotely operated vehicles or it can be derived using well known natural or man-made sources). However, the relative locations of multiple sources detected by the same sensor can be defined.

A key part of the method is the relationship between i_{app} and i. The OBSs directly measure i_{app} [Eq. (1)] but range estimation relies on i [Eq. (4)]. Angle i_{app} is considered to be apparent because the ground velocity in the sediments contains both P- and SV-waves that result from the conversion of acoustic waves at the water-sediments interface. The true emergence angle for P-waves only in the sediments (i_2) is required for the estimation of i and can be derived from i_{app} using standard theory of propagating plane waves at a liquid-solid boundary using Zoeppritz equations (e.g.,

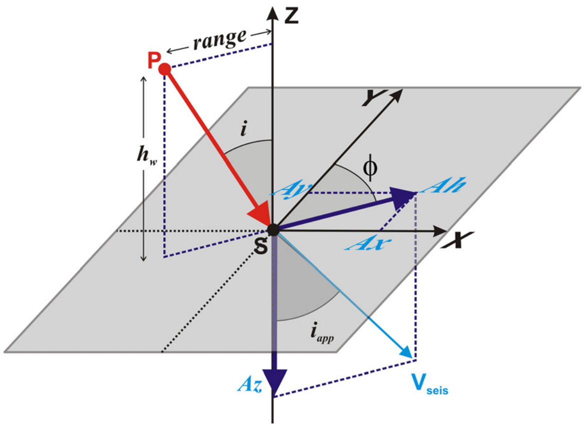

FIG. 1. (Color online) Geometry of the single-station location method as applied to an acoustic source (P) above the seismic sensor (S) at the seafloor. If the wave incidence angle in the water layer (i) and the height above the seafloor of the source (h_w) are known then the horizontal range between the source and sensor can be computed. At the sea-floor the acoustic wave is converted to P- and SV-seismic waves, and the corresponding ground velocity (V_{seis}) is measured by the seismometer. The three components of ground velocity (A_x, A_y, A_z) define the apparent emergence angle in the sediments (i_{app}) and the azimuth (ϕ) of the source. A_h is the horizontal amplitude of the ground motion.

described in Aki and Richards, 1980). These calculations require properties of the water column and sediments to be defined (P-wave velocity in the water column and sediments, SV-wave velocity in the sediments, and water and sediment densities). After obtaining i_2, the incidence angle in the water layer (i) is obtained from Snell's Law of refraction (e.g., Doyle, 1995)

$$i = \sin^{-1}\left(\frac{\alpha_w}{\alpha_s}\sin(i_2)\right), \tag{7}$$

where α_w and α_s are the P-wave velocities for the water layer and sediments, respectively.

B. Measuring the azimuth and apparent emergence angle from seismic data

Seismic signals and fin whale calls have complex waveforms with many cycles. The three-component method presented by Roberts *et al.* (1989) takes the complete waveform of a signal into consideration by using signal cross correlation techniques instead of simple amplitude measurements on the three geophone channels. This method extension is described fully in Roberts *et al.* (1989) and was implemented here, as described in the following text.

The particle velocities recorded by the geophone channels x, y, and z, over time, t, are defined as the vector $\vec{v}(t)$

$$\vec{v}(t) = \begin{bmatrix} \dot{x}(t) \\ \dot{y}(t) \\ \dot{z}(t) \end{bmatrix}. \tag{8}$$

Assuming that the wave is linearly polarized in the ray direction, then particle velocities of the three components should be correlated with constant coefficients c and d that depend exclusively on the azimuth and apparent emergence angle

$$c = \tan(i_{app})\sin(\phi), \tag{9}$$

$$d = \tan(i_{app})\cos(\phi). \tag{10}$$

In addition to the polarized signal, the OBS will also record ambient seismic noise that is assumed to be stationary, uncorrelated to the signal on a given channel and uncorrelated with signals and noise on the other channels in the frequency range studied. The three components of the ground velocity are then expressed as

$$\begin{aligned} \dot{x}(t) &= cP(t) + N_x(t), \\ \dot{y}(t) &= dP(t) + N_y(t), \\ \dot{z}(t) &= P(t) + N_z(t), \end{aligned} \tag{11}$$

where $P(t)$ is the arrival of a pressure wave at time, t, and N_x is a measure of noise on channel x (and similarly for the other channels).

If the cross correlation of two functions f and g are represented by the symbol $\langle f, g\rangle$, then the cross correlation between the x and y particle velocities and the z component will give

$$\begin{aligned} \langle \dot{x}, \dot{z}\rangle &= c\langle P, P\rangle, \\ \langle \dot{y}, \dot{z}\rangle &= d\langle P, P\rangle, \\ \langle \dot{z}, \dot{z}\rangle &= \langle P, P\rangle + \langle N_z, N_z\rangle. \end{aligned} \tag{12}$$

The apparent emergence angle and azimuth are then estimated using

$$i_{app} = \tan^{-1}\left(\frac{\sqrt{\langle \dot{x}, \dot{z}\rangle^2 + \langle \dot{y}, \dot{z}\rangle^2}}{\langle \dot{z}, \dot{z}\rangle - \langle N_z, N_z\rangle}\right), \tag{13}$$

$$\phi = \tan^{-1}\left(\frac{\langle \dot{x}, \dot{z}\rangle}{\langle \dot{y}, \dot{z}\rangle}\right). \tag{14}$$

The three-component method has been implemented in SEISAN, a program for analyzing seismological data (Ottemöller *et al.*, 2011), except for the contribution of the vertical noise autocorrelation [Eq. (12)]. In this case study, the SEISAN routine was used but adjusted to include a measure of the noise autocorrelation.

C. Estimating the incidence angle in the water column

In this case study, the apparent emergence angle (i_{app}) in the sediments was assumed to be approximately the same as the true emergence angle in the sediments (i_2) and was used to estimate the incidence angle in the water (i) directly. This was due to a lack of data about sediment properties in the study region. In the Gulf of Cadiz, field measurements of shallow sediment properties are scarce, but the sediments are known to be water-saturated with P-wave velocities of approximately 1.8 km/s (Shipboard Scientific Party, 1972). SV-wave velocities have not been measured, but the corresponding SV-wave velocity in a fluid-like marine sediment is estimated to be approximately 0.1–0.2 km/s (Buckingham, 1998). A simple simulation study was conducted to show

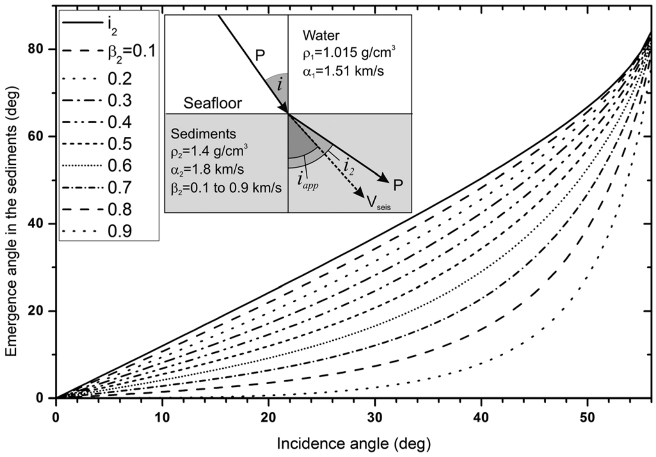

FIG. 2. Simulation results showing angles (both true emergence angles, i_2, and apparent emergence angles, i_{app}) in the sediments plotted against true incidence angles in the water column (i), for a pressure wave produced in the water column (P). The first line corresponds to values of i_2 and each line below corresponds to a set of values for i_{app}, given a particular SV-wave velocity (β_2). The P-wave velocity in the water (ρ_1) is 1.5 km/s, P-wave velocity in the sediments (ρ_2) is 1.8 km/s, water density (α_1) is 1.0 g/cm^3 and sediment density (α_2) is 1.4 g/cm^3. SV-wave velocity ranges from 0.1 to 0.9. The value of i_2 was computed from i by Snell's law and i_{app} was computed by the solution of the Zoeppritz equations. All angles are given in degrees.

that the difference between i_{app} and i_2 is determined by the velocity of the SV-wave (Fig. 2). For a range of known incidence angles, apparent emergence angles were estimated using the Zoeppritz equations for a range of SV-wave velocities (0.1–0.9 km/s, denoted as β_2 in Fig. 2). Water density (ρ_1) and sediment density (ρ_2) were assumed to be 1.015 and 1.4 g/cm^3, respectively. P-wave velocity was assumed to be 1.51 and 1.8 km/s in the water (α_1) and sediment (α_2), respectively. The true emergence angle for the P-wave only, i_2, in the sediment was also calculated using Snell's Law. The results show that assuming i_{app} is equal to i_2 underestimates i to varying degrees. However, the low predicted SV-wave velocity for the study region means that a close relationship between i_{app} and i_2 should exist (Fig. 2), making the use of i_{app} a reasonable approximation in the absence of adequate sediment data.

Not all incidence angles can be estimated by the three-component method. If the P-wave velocity in the second medium (i.e., the sediments in this case) exceeds the P-wave velocity in the first medium (i.e., the water column), then solutions to the Zoeppritz equations can contain complex numbers. The value of the critical angle, i_c, above which complex numbers are calculated, is determined by the exact values of the P-wave velocities

$$\text{for} \quad \alpha_2 > \alpha_1 \quad \sin(i_c) = \frac{\alpha_1}{\alpha_2}. \tag{15}$$

Beyond this critical angle, i_{app} also becomes a complex number that cannot be measured from the OBS. Furthermore, for a given source height above the seafloor, the critical angle can be used to estimate a critical range, R_c, beyond which the three-component method cannot be used,

$$R_c = h_w \tan(i_c). \tag{16}$$

III. STUDY AREA AND SEISMIC ARRAY

Two scientific cruises (one in August 2007 and the other in November 2007) deployed 24 OBSs (22 OBSs were initially deployed in August, followed by further two OBSs in November) as part of the NEAREST (Integrated Observations from Near Shore Sources of Tsunamis: Towards an Early Warning System) project. The main aim of the project was to investigate the characteristics of potential tsunami sources (NEAREST, 2012). The deployment site lay in the Gulf of Cadiz, off the southwest coast of Portugal near the Straits of Gibraltar, in the northeast Atlantic, between approximately 35°N–37°N, and 8°W–12°W (Fig. 3).

The OBSs lay on the seabed in water depths ranging from 1993 to 5100 m with at least 30 km separating a pair of instruments. All instruments were retrieved in August 2008. Each OBS contained a three-component seismometer (model: Guralp CMG-40T, flat velocity response: 0.017–50 Hz) and a hydrophone (model: Hightechinc HTI-04/01/-PCA/ULF, response band: 0.017–8 kHz, sensitivity: −194 dB re. 1 V/μPa). The acquisition system settings ensured that seismic velocity recorded between 0.017 and 40 Hz and pressure recorded from 0.1 to 40 Hz without attenuation. The sampling rate for all channels was 100 Hz (Carrara *et al.*, 2008). The retrieved data for each OBS were saved as four single channel data files in a MiniSEED format, a standard file format for seismological data (Incorporated Research Institutions for Seismology, 2011). The data were filtered between 4 and 40 Hz using a Butterworth eight-pole bandpass filter and were converted to multi-channel sound files using SEISAN (version 8.3) (Ottemöller *et al.* 2011). The hydrophone data were also used to create single channel .wav files (in a 32-bit integer format, filtered between 2 and 50 Hz using a Butterworth eight-pole bandpass filter).

IV. VALIDATION ANALYSIS: AIRGUN DATA

In September 2007, the ship R/V Atalante passed over OBS18 and OBS19 while producing airgun shots (Somoza *et al.*, 2007). The results of the three-component analysis from data recorded by each OBS were similar; hence, for brevity, the results from OBS18 are presented in detail and a summary of the results from OBS19 are given. A subsample of the dataset was used for the validation study presented here: when the ship was within 12 km of OBS18 and OBS19 for approximately 2.5 and 2.3 h, respectively. The depth of OBS18 was 4605 m and the depth of OBS19 was 4287 m. A normalized cross correlation algorithm to detect airgun shots in both datasets was run in SEISAN using manually selected airgun pulse templates (one for each dataset). The templates were selected by displaying the waveform of the datasets and the first pulse of a direct wave with a good signal to noise ratio (SNR) was identified in each dataset (Fig. 4). The templates were chosen on the vertical channel, z, and all subsequent detections were made using the same channel. The template airgun shots were broadband signals, covering the frequency range of the OBSs. The duration of the template selected in the OBS18 dataset was 430 ms (Fig. 4) and the duration of the OBS19 template was 370 ms.

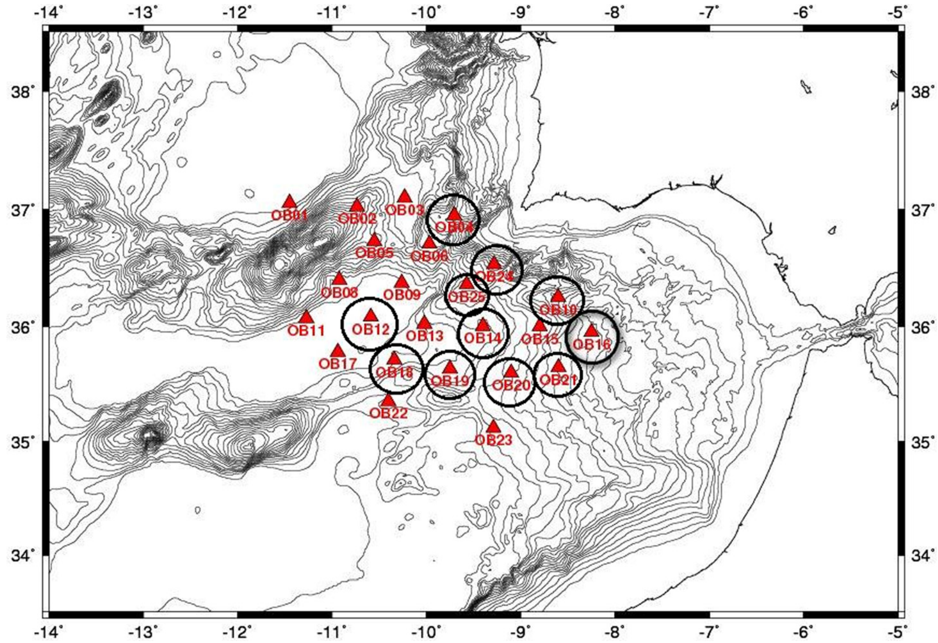

FIG. 3. (Color online) Location of an array of 24 ocean bottom seismometers (OBSs) off the south coast of Portugal. The circled OBSs are those that could be used for the distance sampling analysis. OBS7 is missing from the map because very limited data were retrieved from this instrument.

A. Preliminary analysis

For the analyses of data from both OBSs, a threshold was set for the cross correlation to minimize the risk of false detections—if the correlation between the template and a signal in the dataset did not exceed the threshold value, then the detection of that signal was discarded. The threshold was set to 0.5 (1.0 would indicate a perfect correlation). In

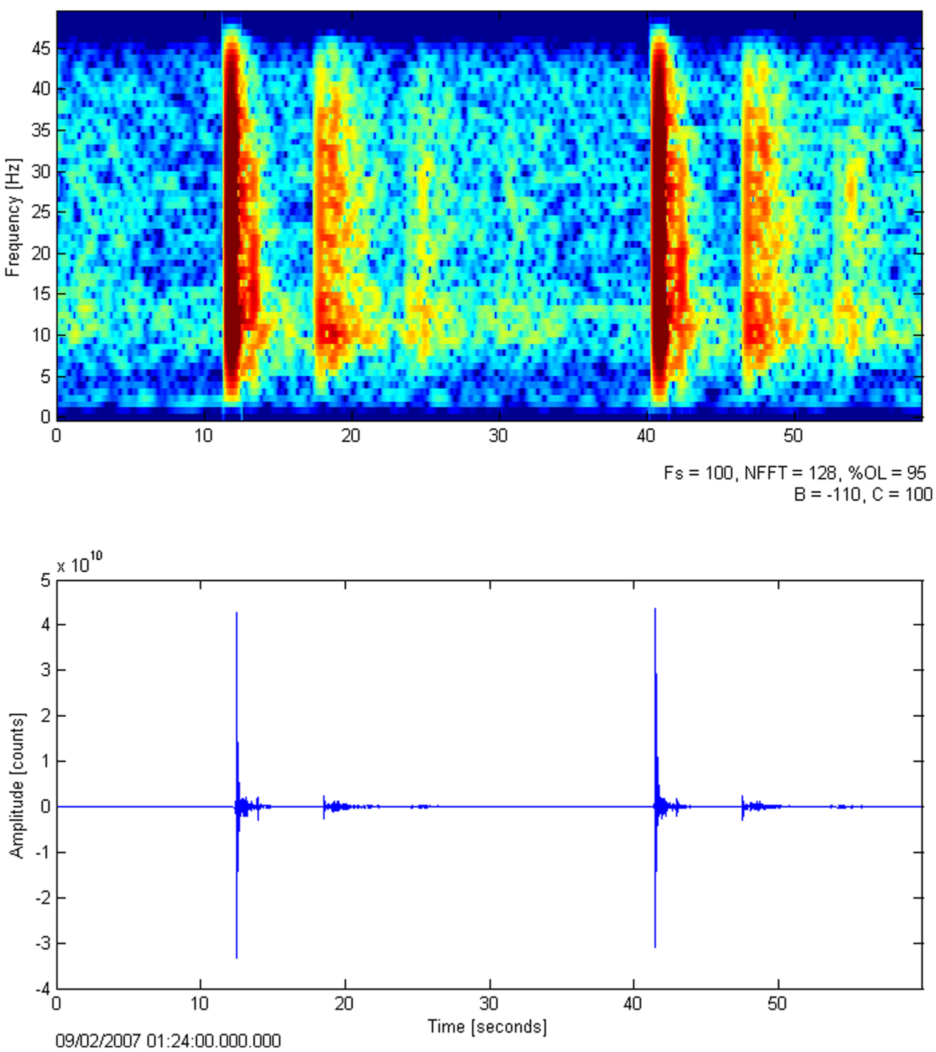

FIG. 4. (Color online) Top: A spectrogram showing 60 s of data from OBS18 on September 2, 2007. Spectrogram parameters: Frame size—128 samples, 95% overlap, Hanning window, not equalized. Two airgun shots are visible plus multipath arrivals. Bottom: The same data viewed as a waveform (amplitude plotted against time). The first displayed shot was used as the template call for automatic detection of other airgun shots in the OBS18 dataset.

addition, a 1 s minimum buffer period between successive detections was set to prevent the cross correlation routine triggering on the same signal more than once. If a second detection was encountered within 1 s of another detection, the detection with the highest correlation value was selected. The times of all detected signals were stored in SEISAN.

The three-component analysis was applied, assuming that the P-wave velocity in the sediments was 1.8 and 1.5 km/s in the water column. For these velocity values, the estimated critical incidence angle was 56°, resulting in an estimated critical range of 6.9 km for OBS18 and 6.5 km for OBS19. To correct for noise, a window of noise equaling the length of the template signal was measured immediately prior to a detection. A total of 287 airgun shots were produced in the OBS18 dataset and 120 signals were detected, which were all verified to be airgun shots by visually inspecting the spectrogram. One signal had to be discarded for further analysis as data for its location were missing.

The known ranges between the remaining 119 signals and the OBS were compared to the estimated ranges. The ship moved toward the OBS, then away from the instrument. Range was well estimated for signals produced during the ship's approach, but range was increasingly poorly estimated as the ship moved away [Fig. 5(a)]. The range was underestimated for 96 signals and overestimated for 23 signals. The maximum difference between the known range and the estimated range was 5.4 km. The poorer estimates of range were reflected in the azimuth and incidence angle estimates. The known azimuths had to be corrected by a constant to account for the unknown orientation of the OBSs so that they could be compared to the estimated azimuths. The estimated values matched the corrected known values reasonably well at ranges up to approximately 5 km, but there were some

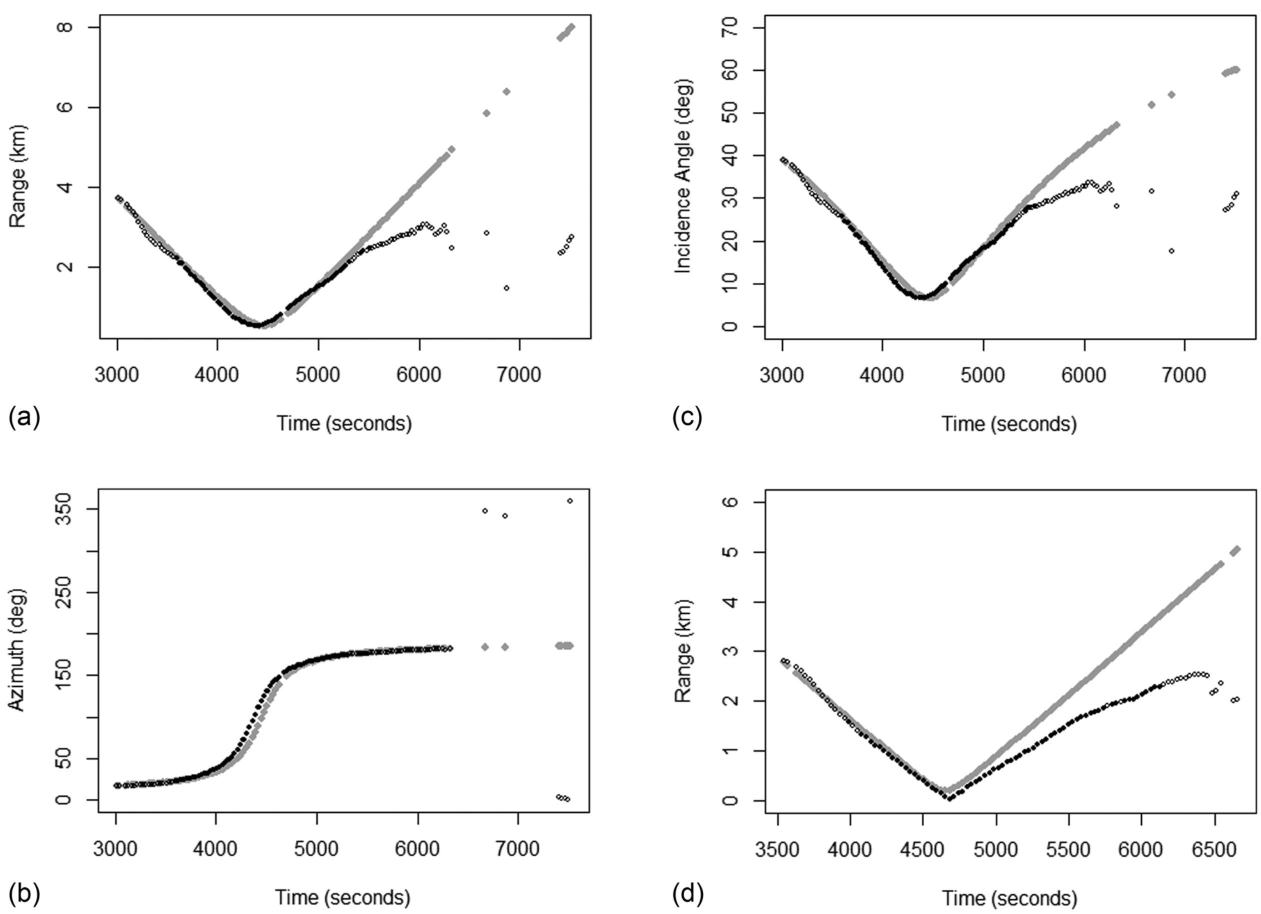

FIG. 5. (a) Estimated horizontal range (black circles, both closed and open) compared to the known range of airgun shots (gray closed circles) recorded on OBS18 through time (displayed as number of seconds since 00:10:00 on September 2, 2007, which was the start of the period containing airgun shots used in this analysis). Black open circles denote estimated ranges of airgun shots detected in the preliminary analysis. Range estimates retained once selection criteria were applied to filter out poor locations are denoted by black closed circles. All ranges are given in kilometers. (b) Estimated azimuths (black circles, both closed and open) compared to the known azimuths of airgun shots (gray closed circles) recorded on OBS18 through time (displayed as number of seconds since 00:10:00 on September 2, 2007, which was the start of the period containing airgun shots used in this analysis). Black open circles denote estimated azimuths of airgun shots detected in the preliminary analysis. Azimuth estimates retained once selection criteria were applied to filter out poor locations are denoted by black closed circles. All azimuths are given in degrees. (c) Estimated incidence angles (black circles, both closed and open) compared to the known incidence angles of airgun shots (gray closed circles) recorded on OBS18 through time (displayed as number of seconds since 00:10:00 on September 2, 2007, which was the start of the period containing airgun shots used in this analysis). Black open circles denote estimated incidence angles of airgun shots detected in the preliminary analysis. Incidence angle estimates retained once selection criteria were applied to filter out poor locations are denoted by black closed circles. All angles are given in degrees. (d) Estimated horizontal range (black circles, both closed and open) compared to the known range of airgun shots (gray closed circles) recorded on OBS19 through time (displayed as number of seconds since 06:00:00 on September 2, 2007, which was the start of the period containing airgun shots used in this analysis). Black open circles denote estimated ranges of airgun shots detected in the preliminary analysis. Range estimates retained once selection criteria were applied to filter out poor locations are denoted by black closed circles. All ranges are given in kilometers.

large differences at greater ranges [Figs. 5(a) and 5(b)]. The known and estimated incidence angles were also compared. The incidence angles were well estimated within 4 km, but they became poorer as the ship moved away from the OBS [Figs. 5(a) and 5(c)]. The last five detected airgun shots were outside the critical range, and so the estimates of azimuth and incidence angle were expected to be poor. However, there were two airgun shots within the critical range (at 5.8 and 6.4 km) that also produced very poor azimuth and incidence angle estimates.

A total of 281 airgun shots were produced in the OBS19 dataset and 102 of these were detected. The estimated range reflected the true range well on the ship's approach, but, again, range estimation was poorer as the ship moved away from the instrument. This effect was generally more pronounced for this dataset although the maximum difference between known and estimated range (3.0 km) was less than in the OBS18 dataset [Fig. 5(d)].

B. Analysis with selection criteria

The localization results were filtered using several criteria in an attempt to retain only good quality localizations. The detection threshold was raised to 0.75, and the SNR of each detection was calculated and had to exceed a threshold (set to 5). The relationship between the two vertical channels (channels h and z) also enabled poor quality localizations to be discarded as follows. The correlation and time difference between the signals recorded on the two channels were measured and compared against thresholds. The correlation threshold was set to 0.3, and the maximum allowable time difference was 0.1 s. The application of these criteria to the OBS18 dataset removed 41 signals, including the more distant ones, and the azimuths were well estimated for the remaining 79 signals [Fig. 5(b)]. The incidence angle was still poorly estimated for some signals as the ship moved away from the instrument [Fig. 5(c)], but the maximum difference between the known range and estimated range was reduced to 894 m. Range was underestimated for 60 signals and overestimated for 19 signals [Fig. 5(a)]. The majority of the range differences were within 200 m (for 64 signals).

The same criteria were applied to the OBS19 dataset and 34 signals were removed. The filtered results still contained poor range estimates as the ship moved away from the OBS, and this was reflected in both the maximum difference between the known range and estimated range (1.4 km) and that only 30 of the 68 remaining signals had a range difference of less than 200 m [Fig. 5(d)].

Aside from the apparent ship movement effect, these selection criteria worked well in removing many of the problematic estimates at larger ranges, although further analyses are required to assess the exact role of each criterion. In addition, the results suggest that using the apparent emergence angle in the sediments is, in most cases, a reasonable approximation for the true emergence angle in the sediments. Whether the approximation is a contributing factor to the poorer estimates of the incidence angle in the water column is not known. Further discussion of the potential sources of bias and improvements to the method is given in Sec. VII.

V. ECOLOGICAL APPLICATION: FIN WHALE DATA

A. Fin whale distribution and acoustic behavior in the northeast Atlantic

Fin whales occur worldwide and are categorized as "endangered" on the International Union for Conservation of Nature's Red List of Threatened Species (Reilly *et al.*, 2008). Fin whales are found in both the Mediterranean Sea (Notarbartolo di Sciara *et al.*, 2003) and the northeast Atlantic (e.g., Nieukirk *et al.*, 2004; Charif and Clark, 2009). Studies have used tagging, genetics, visual, and acoustic surveys to try to establish the population structure and distribution of fin whales in this area (Castellote *et al.*, 2012).

Fin whales produce a variety of sounds (Thompson *et al.*, 1992). The "20-Hz" call is the most studied fin whale vocalization and has been recorded worldwide e.g., in the Pacific, the Atlantic and the Southern Ocean (Širović *et al.*, 2007; Stafford *et al.*, 2009; Nieukirk *et al.*, 2012). The calls may be produced in long, stereotyped bouts, which are often referred to as song (Janik, 2009). To date, only males have been found to sing, and it is possible that the song is part of a reproductive strategy (Croll *et al.*, 2002). Each call is $\sim$1 s in duration, sweeping downward over a 15–30 Hz range. Source levels above 180 dB re. 1 μPa at 1 m have been estimated (e.g., Watkins *et al.*, 1987). There is geographic variation in some features of the calls, such as frequency content and inter-call intervals, which may indicate population level differences (e.g., Delarue *et al.*, 2009, Širović *et al.*, 2007).

Between 2006 and 2009, acoustic data were collected from various sites within the Mediterranean Sea and in the Atlantic Ocean (Castellote *et al.*, 2012). Castellote *et al.* (2012) found that the inter-call interval, the duration, and the frequency bandwidth of calls produced in the Atlantic were significantly different to calls produced in the Mediterranean Sea. Calls detected in the Straits of Gibraltar and the Alboran Sea (the first stretch of Mediterranean water to the east of the Straits) matched the call type associated with Atlantic Ocean fin whales. The Mediterranean call type was not detected in this region. The authors concluded that whales from the Atlantic migrate into the Mediterranean Sea during the winter but that Mediterranean whales may not leave the Mediterranean Sea (Castellote *et al.*, 2012). The area where the OBS array in this study was deployed may therefore be part of the migration route for animals moving between the Atlantic Ocean and the Mediterranean Sea. The OBS array provides a valuable dataset of vocalizations over the course of 12 months. Furthermore, the ability to estimate distances to calls means that distance sampling (Buckland *et al.*, 2001) can be used to estimate the average probability of detecting a call, a key parameter for estimating animal abundance using passive acoustic data. The current population size for fin whales in the central and northeastern Atlantic is estimated to be 30 000 (approximate 95% confidence interval: 23 000–39 000) (International Whaling Commission, 2010), but it is not known how many animals use the Straits of Gibraltar as a migratory corridor.

Although a year of data were collected from this array, the detection and distance sampling analysis of fin whale calls reported here was performed on data collected on only a single day as proof of concept. However, this study is part of a larger research effort, which aims to produce density estimates of fin whales across the monitored region using the OBS data.

B. Detection and range estimation of fin whale calls

The detection and range estimation protocol for the fin whale call analysis was similar to that used in the airgun shot analysis. To pick a template call with a good SNR, spectrograms were created from the .wav files and viewed using TRITON (Wiggins, 2003), a software package written in MATLAB (Mathworks, 2012). Spectrograms in TRITON were calculated using a discrete Fourier transform with a Hanning window (using a window length of 128 samples with an overlap of 95%) (Lurton, 2002). Brightness and contrast settings were adjusted to produce the best visual image. Each viewing window was set to display 30 s of data and was equalized over the 30 s window to improve the SNR. The entire frequency range (0–50 Hz) was displayed for all spectrograms (Fig. 6). The template call was chosen from a recording on instrument OBS04 on January 4, 2008. It ranged in frequency from 27 to 18 Hz and had a duration of 790 ms (Fig. 6).

The cross correlation threshold was set to 0.75, and a 1 s buffer period was defined. The three-component analysis was applied, assuming that all calling whales were situated at the sea surface. The same P-wave velocities in the water and sediment were assumed as in the airgun shot analysis, and the same criteria were used to select the localizations: the SNR had to be greater than 5, the correlation between the detections recorded on the two vertical channels had to be greater than 0.3, and the time difference less than 0.1 s.

Not all OBSs could be used for the localization of fin whale calls because some of the horizontal geophones failed at various times. On January 4, 2008, the channels required for call localization were available on 11 OBS instruments (Fig. 3). Running the cross correlation detector and conducting the three-component analysis on the available data resulted in a total of 2340 localizations of acceptable quality (Table I). The ability of the automatic detector was assessed by manually checking over 10% of the detections ($n = 260$): 95% of detections were positively identified as fin whale calls. The remaining 12 detections were not definite false detections but could not be positively identified as fin whale calls.

Estimated azimuths ranged from 0° to 359.9°, and estimated incidence angles ranged between 2° and 49°. The maximum estimated horizontal range of a call from an OBS was 3773 m, and the minimum was 87 m. Therefore due to the wide spacing of the OBSs, none of the detections were duplicates. The spatial distribution of detected calls around each OBS is given in Fig. 7. Note that the displayed orientation is arbitrary because the absolute orientation of the calls with respect to each OBS is not known.

VI. DISTANCE SAMPLING ANALYSIS

A. Density estimation using passive acoustic data

The potential of passive acoustic monitoring to estimate cetacean density and abundance has been known for many years (e.g., McDonald and Fox, 1999). Estimates of the minimum number of whales, minimum whale density, and relative abundance in particular areas based on such data have appeared in several studies (e.g., McDonald and Fox, 1999; Charif *et al.*, 2001; Gillespie *et al.*, 2005; McDonald, 2006). In recent years, there have been large advances in the application and development of statistical methods to estimate absolute density and abundance of cetaceans using passive acoustic surveys (reviewed in Marques *et al.*, 2013). The suite of available methods include plot sampling (Moretti *et al.*, 2010; Ward *et al.*, 2012), distance sampling [both line transect sampling with towed instruments (e.g., Barlow and Taylor, 2005) and point transect sampling with fixed (i.e., static) instruments (e.g., Marques *et al.*, 2011)], spatially explicit capture-recapture (SECR) (Marques *et al.*, 2012; Martin *et al.*, 2013) and a range of novel approaches developed specifically for this purpose (e.g., Marques *et al.*, 2009).

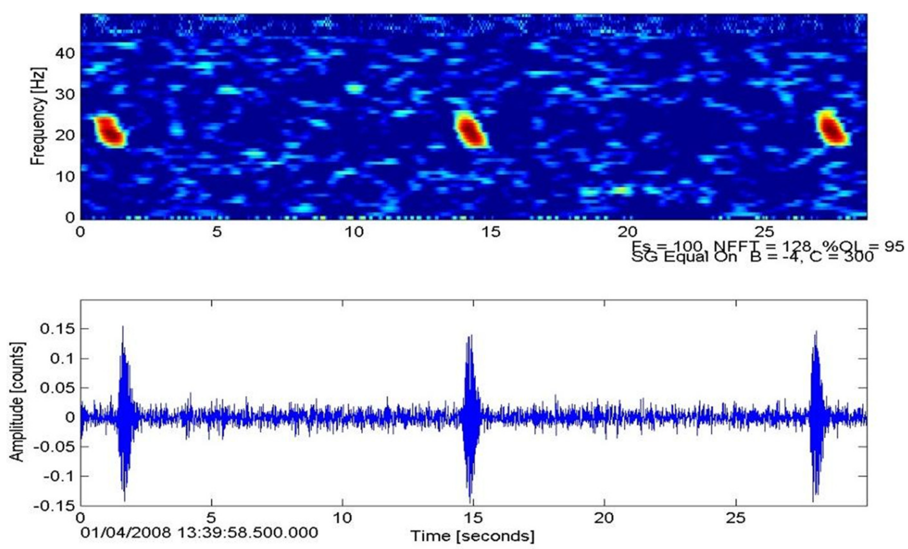

FIG. 6. (Color online) Top: A spectrogram showing 30 s of data from OBS04 on January 4, 2008. Spectrogram parameters: Frame size—128 samples, 95% overlap, Hanning window, equalized. Three fin whale calls are visible. Bottom: The same data viewed as a waveform (amplitude plotted against time). The first call displayed was used as the template call for automatic detection of other calls.

TABLE I. Detections of fin whale calls for each OBS instrument, detected over 24 h.

OBS	04	10	12	14	16	18	19	20	21	24	25	Total
No. detections	550	713	0	0	264	0	96	516	67	1	133	2340

To generate estimates of absolute density and abundance, any undetected animals must be accounted for (both vocalizing and non-vocalizing in an acoustics context). This requires an estimate of the average probability of detecting the acoustic signal that is being used; this corrects for signals that were produced by an animal but missed by the detection process. Furthermore, an estimate of the average rate at which the signal is produced over the time surveyed (hereafter referred to as the cue rate) is also required unless individual animals can be identified from their signals. This latter parameter is used to convert the estimate of the density or abundance of signals to an estimate of the density or abundance of animals. It can also be used to account for animals that are not vocalizing at the time of the survey (see Marques *et al.*, 2013).

A typical example of a formula used to estimate density of animals from detected acoustic signals is

$$\hat{D} = \frac{n(1-\hat{c}_{fd})}{\pi w^2 \hat{P}_{\mathrm{det}} T \hat{r}_{\mathrm{cue}}}, \tag{17}$$

where n is the number of detected cues, $\hat{c}_{fd}$ is the proportion of false detections (measured manually from a sample of the detections), w is the truncation distance (see following text), $\hat{P}_{\mathrm{det}}$ is the average probability that a cue made in the surveyed region will be detected, T is the total monitoring time, summed across all instruments and $\hat{r}_{\mathrm{cue}}$ is the cue rate. Animal abundance in a given area is estimated by multiplying the density estimate by the area of interest (Buckland *et al.*, 2001).

In this case study, the probability of detection was estimated using distance sampling, but no appropriate estimate of the cue rate was available to convert this to an estimate of animal density or abundance.

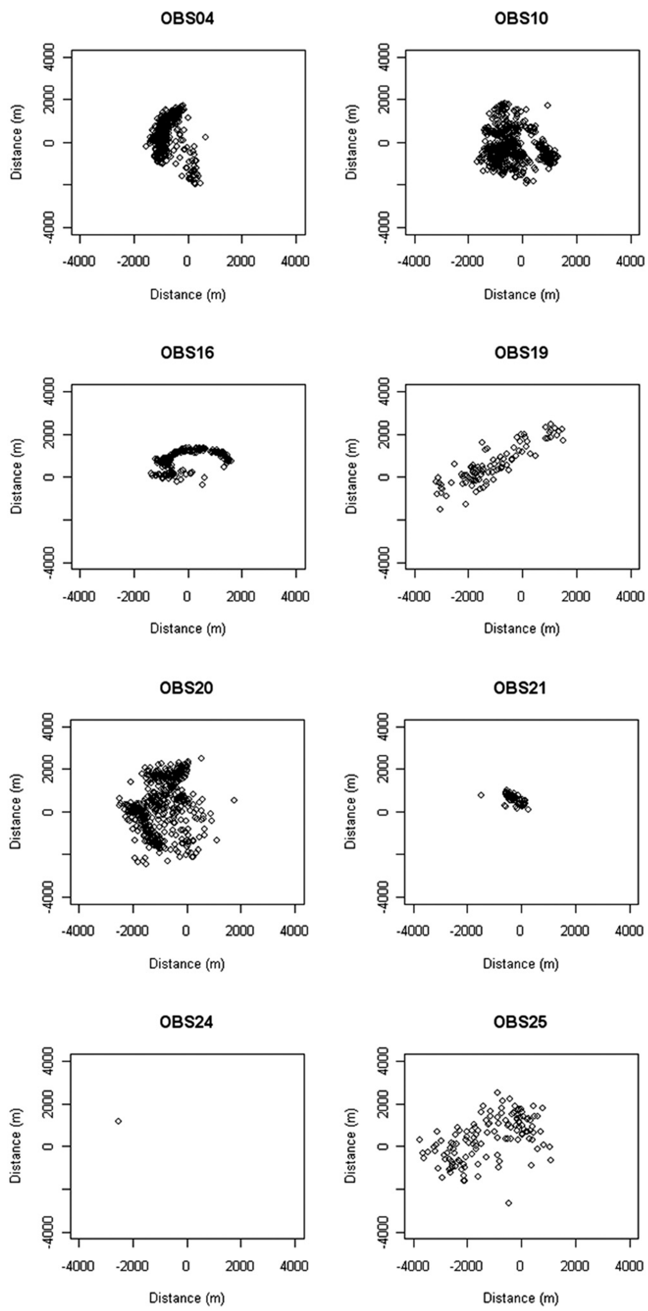

FIG. 7. Relative positions of presumed fin whale calls (m) plotted around separate OBS instruments (all OBS instruments are located in the center of each plot at 0, 0). The absolute location of the calls is unknown due to the unknown orientation of the horizontal geophones.

B. Distance sampling—background and assumptions

In distance sampling, a statistical model, known as the detection function, is fitted to the horizontal distances to detected individual animals (or cues) to estimate the average probability of detecting an animal (or cue) as a function of distance (Buckland *et al.*, 2001). Distance sampling based on cues requires several assumptions, which need to be upheld to provide a robust estimate of the average probability of detection and associated variance. The key assumptions are

(1) Cues made on the track line (for surveys conducted along transect lines) or at the center of the point (for surveys conducted using a static observer or instrument) must be detected with certainty. In this case study, that implies that all calls made directly above each OBS must be detected.
(2) Distances to cues are measured accurately.

A third assumption is that detections of cues are independent from one another, but the methods are robust to violation of this, although statistical tests to assess the fit of the detection function may be affected if there is strong dependence between detections (Buckland *et al.*, 2001). In addition, dependent detections may cause overdispersion in the distance estimates, leading to the selection of an over-complicated detection function. We discuss whether the two key assumptions were met in this analysis in Sec. VII.

C. Estimating the probability of detecting a fin whale call, P_{det}

The number of detections with accepted locations was 2340 (including any uncertain detections; see Sec. VII). The distribution of estimated horizontal ranges (Fig. 8) was typical of distance sampling data around fixed points: the frequency of detections increased then decreased with range because the area around points increases with range, therefore incorporating an increasing number of signals, but signals become more difficult to detect as range increases (see Buckland *et al.*, 2001, Sec. 5.2 and Fig. 5.1).

The distance sampling analysis was conducted using PROGRAM DISTANCE (version 6.1, beta 1) (Thomas *et al.*, 2010) and followed guidelines given in Buckland *et al.* (2001). As part of the initial modeling, a truncation distance, w, was chosen (3000 m), and all calls detected at a distance greater than 3 km (approximately 1% of all observations) were discarded (leaving 2321 detections). This improves the reliability of the detection function fitting (see Buckland *et al.*, 2001 for details). Three different detection function models were fitted to the remaining data: a half normal key function, the key function with up to three cosine adjustment parameters, and the key function with up to three hermite polynomial adjustment parameters. Akaike's Information Criterion (AIC) was used to choose the most parsimonious model, indicated by the lowest AIC score among competing models. The absolute goodness of fit of the selected model was judged by visually inspecting the fit of the model to the data and the quantile–quantile (Q-Q) plot (points lining up on a 1:1 line on the Q-Q plot suggest a good fit). The result of the Cramer–von Mises goodness of fit test (conducted using PROGRAM DISTANCE) was also considered. The null hypothesis of the goodness of fit test (supported by a high p value) is that the fitted model is the true model (Buckland *et al.*, 2001, 2004).

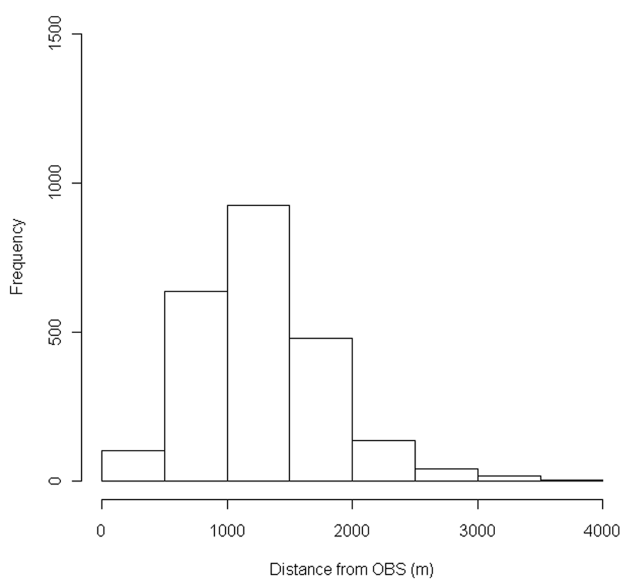

FIG. 8. Horizontal ranges (m) of presumed fin whale calls from eight OBS instruments estimated using the three-component analysis. The total number of accepted ranges estimated was 2340.

The fit of the selected detection function, a half normal key function with two cosine adjustment parameters, was reasonable (Fig. 9). The fit of the detection function to the data at ranges close to the OBS is particularly important because the gradient of the detection function at zero distance has a large influence on the estimate of P_{det}. There was some lack of fit at small ranges, which was evident in both the detection function and Q-Q plots (Figs. 9 and 10). The goodness of fit test had a p value ≤ 0.001, suggesting that there was strong evidence to reject the null hypothesis. However, such goodness of fit tests are sensitive to large datasets and so can suggest a bad model fit, even when the fit is adequate. In addition, all detections were not independent from each other (discussed in Sec. VII); this may also affect the goodness of fit test results. The estimate of P_{det} within the truncation distance was 0.313 (standard error: 0.033).

VII. DISCUSSION

A. Assumptions of the three-component analysis

A number of simplifications of the single-station location method were used in its application to the airgun shot and whale call datasets: (a) The effect of SV-wave velocity in the sediments was neglected, and the incidence angle in the water layer was computed directly from Snell's law (it was assumed that the apparent emergence angle was close to the true emergence angle in the sediments); (b) it was assumed that all OBSs were placed on water saturated sediment with the same P-wave velocity; (c) seismic noise was assumed to be random and uncorrelated with signals and noise on other channels; (d) a homogenous vertical sound velocity profile was assumed to estimate the horizontal range i.e., acoustic rays were assumed to travel in straight lines in the water; (e) finally, all calling whales were assumed to be at the sea surface.

The relationship between the apparent and true emergence angles in the sediments was investigated prior to the airgun validation study using a simulation study as discussed in Sec. II C. This suggested that the apparent angle was an adequate approximation for the true emergence angle in this preliminary work. However, incidence angles in the water column and ranges will have been underestimated by ignoring the contribution of SV-waves to the apparent angle. A future step in this work will be to use the best estimates of sediment properties for the study region and apply the Zoeppritz equations. The shallow marine sediments in the Gulf of Cadiz should be similar to pelagic sediments in other parts of the world as indicated by available empirical data (Shipboard Scientific Party, 1972). Furthermore, all OBSs were deployed in a similar geological environment, and so it is not expected that there will be large differences in sediment properties between instruments. It will be difficult to test the assumptions made about seismic noise and their possible effects on the range and azimuth estimates. However, only detections with good SNR are selected, and, for these detections, the noise contribution will be small.

The assumed water column properties will have two effects on the range estimates. First, the incidence angle derived by Snell's law or the Zoeppritz equations depends

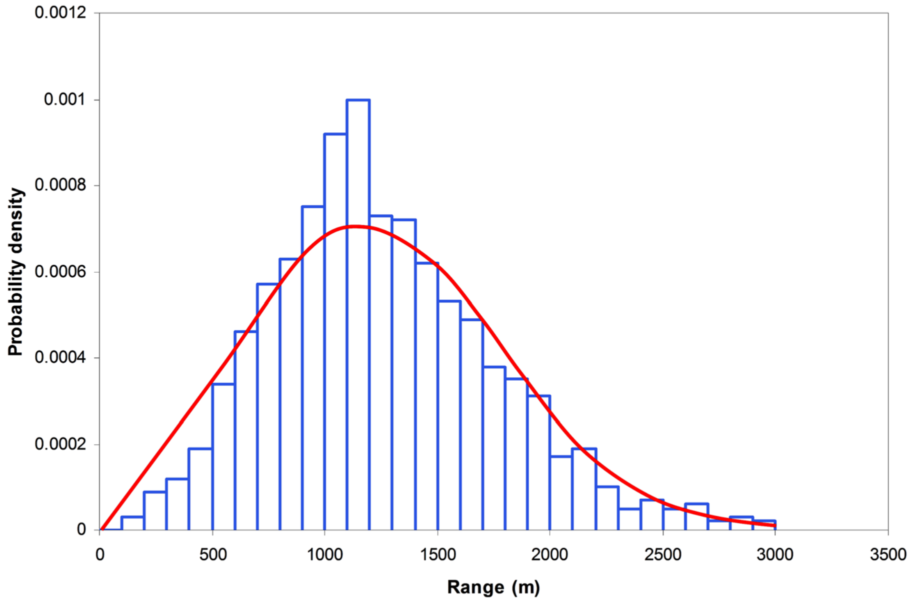

FIG. 9. (Color online) The fitted detection function (plotted as a probability density function) with a histogram of the observed horizontal ranges of the detections (*m*). The frequencies of the histogram have been scaled accordingly.

on the true sound speed immediately above the OBS. Given that different OBSs are at different water depths, the sound speed is unlikely to be constant for all of them. Second, sound velocity is affected by depth, temperature, and salinity, all of which show spatial and temporal variation (Lurton, 2002). Therefore an important improvement to this method would be to use appropriate sound velocity profiles for each OBS and apply a ray tracing model to more accurately predict the location of the source (e.g., Lurton, 2002). However, we do not expect the incorporation of a realistic sound velocity profile to have a large effect on range estimation. Preliminary work with the airgun datasets suggests that the bias in range estimation is less than 200 m within the critical range.

Assuming the same depth for all calling fin whales was another simplification. However, although fin whales are able to dive to depths of over 400 m (Panigada *et al.*, 2003), calling whales have been recorded at approximately 50 m (Watkins *et al.*, 1987). Therefore the assumption that calling fin whales were at the sea surface seemed reasonable for this preliminary study, especially as the OBSs were deployed in deep water, so the relative inaccuracy in the estimated horizontal distances caused by imprecision in the assumed depths of the animals will be small.

B. Performance of the three-component analysis in the validation study

The preceding assumptions (apart from whale depth) were broadly tested by performing a validation exercise of the three-component analysis using airgun sounds of known location. In general, the method performed well, especially when selection criteria were used and ranges were restricted to be smaller than the critical range. Most horizontal ranges

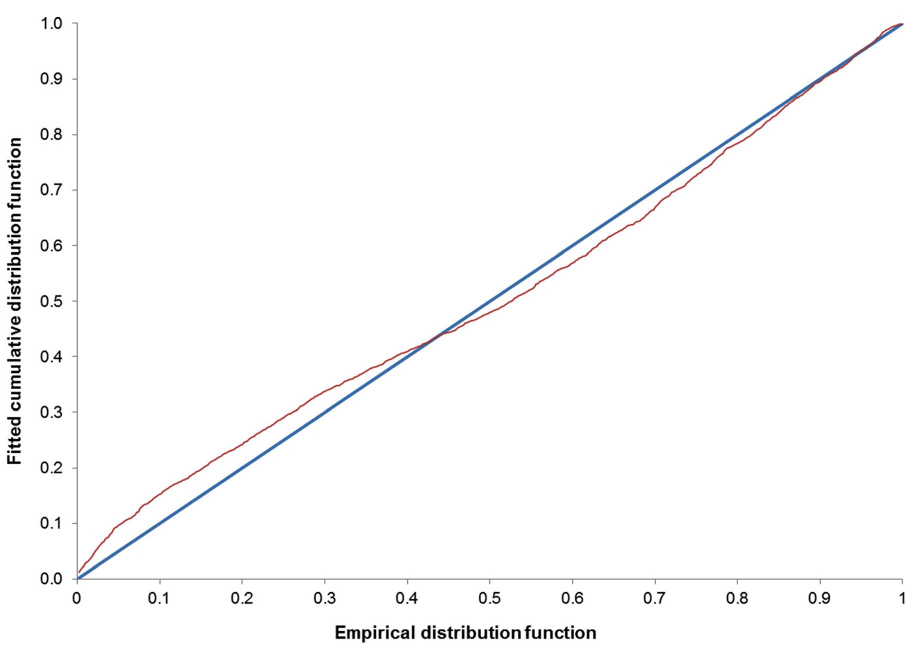

FIG. 10. (Color online) Quantile-quantile plot to assess the goodness of fit of the detection function model. A good model fit is indicated if the observed data points (forming the thin curved line) line up along the 1:1 line (the thick straight line).

were then estimated with a bias of up to 200 m but range underestimation (up to 1400 m) persisted.

The method would also benefit from a validation exercise using fin whale calls, and we plan to undertake this. Although airgun shots are produced at the sea surface, they differ from fin whale calls in their duration, frequency range, and structure. Furthermore, the shots generally had a higher SNR than the whale calls, and their propagation through the water column may have been different. To establish whether the three-component analysis requires further modification for specific use on fin whale calls, a dataset from an OBS array with smaller instrument spacing will be analyzed using both standard multiple-instrument localization methods and the three-component method.

C. Further development of the three-component analysis

In addition to checking the method's assumptions and further validation work, the selection criteria require further investigation. Three criteria were used to filter the locations (SNR and the correlation and time difference between the two vertical channels), but the values selected for these criteria failed to remove all poor estimates. Further work needs to be done to determine whether the performance of the method could be improved using different parameter values or additional criteria. For example, a parameter estimated in the three-component analysis, the coherency factor, should provide a quality check of both the azimuth and incidence angle estimates (Roberts *et al.*, 1989). However, in preliminary trials, using the coherency factor was found to eliminate otherwise good locations at closer ranges.

D. Detection and range estimation of fin whale calls

The cross correlation routine used to detect fin whale calls worked well. None of the sampled detections were definitely false, and 95% of sampled detections were classified as definite fin whale calls. The remaining 5% were "uncertain" detections. In a density analysis where the number of detections is used [Eq. (7)], the analyst would have to decide whether to include uncertain detections as calls or false detections or rerun the analysis using a higher detection threshold, which would hopefully eliminate such uncertain detections. Further removal of calls by changing the threshold or selection criteria will not negatively affect the subsequent distance sampling analysis, as long as the sample size of detected calls does not become too low and that calls produced immediately over the OBS (at 0 m horizontal distance) are not filtered out.

The validation study demonstrated that there is error in the estimation of the incidence angle and range (and, to a lesser extent, the azimuth). Therefore it is likely that the locations of fin whale calls contain error, but this will be addressed by improving the assumptions of the method and performing a validation study using fin whale calls. Furthermore, the unknown orientation of the OBSs was not an issue in this study as only range from each OBS to each calling fin whale was required for the distance sampling analysis. However, knowledge of the absolute location of each animal would aid other research topics, e.g., investigations of animal movement in relation to oceanographic features.

E. Distance sampling using single OBSs

OBS arrays have been used in previous cetacean studies (e.g., Rebull *et al.*, 2006; Dunn and Hernandez, 2009; Wilcock and Thomson, 2010), but this is the first attempt to apply distance sampling techniques to data from OBSs. Given that propagation modeling studies have shown that fin whale calls can be detected up to ~50 km (Širović *et al.*, 2007; Stafford *et al.*, 2007), the estimate of P_{det} might appear to be lower than expected for a 3 km monitoring radius. However, the estimate of P_{det} is the estimated probability that a given call was not only detected but also produced a localization of sufficient quality. We next consider whether the assumptions that underpin the distance sampling approach were reasonable.

The main assumptions associated with distance sampling analyses based on cue counting are listed in Sec. VI B. Fin whale calls have high source levels, and so it was reasonable to assume that an animal calling at a horizontal range of 0 m, i.e., directly above an OBS will be detected. The results from the airgun validation study suggested that the three-component method tends to underestimate the range to sound sources. In distance sampling, this will lead to an underestimate of P_{det} and an overestimate of density. Therefore the true probability of detecting a whale call within 3 km might be higher than the estimated value of 0.3. Fin whales can produce calls in long bouts, so the assumption of independent distances was clearly violated for distances that were estimated within the same song bout. As a result, despite detecting over 2000 calls, the density estimation analysis suffered from having a small number of independent distance estimates. However, distance sampling is robust to dependent detections. The distances were not overdispersed, though the goodness of fit test may have been affected.

F. Improvements to the distance sampling analysis—toward density estimation

In this analysis, we have modeled the probability of detecting a call as a function of range from the instruments. One potential extension is to use multiple covariate distance sampling (MCDS), which allows other covariates that potentially influence cue detectability to be included (Marques *et al.*, 2007). For example, in some visual surveys, different sea states or observer identity may affect the probability of detecting an animal or cue, and these can be included as covariates in the detection function. In acoustic surveys, ambient noise is an important covariate to consider, especially if a survey takes place over extended spatial and temporal scales; we plan to do so in future analyses.

Due to the lack of an appropriate cue rate, it was not possible to estimate animal density or abundance in this analysis. The cue rate required for density or abundance estimation is a measure of how often an animal vocalizes on average during a time interval that includes periods of both vocal and non-vocal activity. The cue rate is, therefore, a difficult parameter to estimate accurately. Ideally, it should be estimated using data from tagged animals or from animals that are tracked both visually and acoustically to capture non-vocal activity. In addition, the cue rate should be measured at the same time and in the same region as the main study. Tagging studies of fin whales have been conducted elsewhere (Southall *et al.*, 2011), so a relevant cue rate may be available in the future. If individual-based distance sampling could be used (rather than cue counting) where detections of animals, not calls, are recorded, the need for a cue rate would be eliminated. However, identifying individual tracks would require a more detailed analysis of the timing of the detections and may be too difficult in periods where there is a lot of vocal activity.

Another important consideration for density or abundance estimation is the correction for false detections and other features of the automatic detector that may cause bias. Equation (7) provides a correction for false detections $(1-\hat{c}_{fd})$. For fin whale calls, multipath arrivals of calls are also a potential issue. They may trigger the detector, resulting in one call being counted multiple times. Multipath signals can be dealt with by setting the buffer parameter to exclude potential multipath arrivals or by checking a sample of detections to determine the proportion of multipath arrivals in the sample in the same way as for false positives. The latter is likely to be the most effective option as extending the buffer period could exclude calls from other individuals. In addition, multipath arrivals can have a higher amplitude than the main signal, so multipath arrivals may be hard to exclude using automatic methods (Wilcock and Thomson, 2010).

G. Conclusions

We have shown that data from OBS arrays have the potential to produce density and abundance estimates of marine mammals that produce low frequency vocalizations. Although the three-component method can only localize calls within a certain critical range, the ability to create a widely spaced, or sparse, array from instruments that can each range to calling whales is advantageous. First, each instrument acts as an independent monitoring point. In contrast, monitoring points would have to consist of several instruments if multiple-instrument localization methods were to be used to produce ranges for distance sampling. Second, the accuracy and precision of density estimates are improved with a larger number of monitoring points (Buckland *et al.*, 2001). Therefore sparse arrays of OBSs, or similar instruments, have the potential to monitor larger survey regions and produce more robust results for the same cost as arrays that have the same number of instruments but rely on close instrument spacing for range estimation. Many OBS arrays have been deployed in the past, and more deployments are planned for the future (U.S. National Ocean Bottom Seismography Instrument Pool, 2010). There are, therefore, plenty of opportunities for these arrays to be used to monitor marine mammal populations. However, regardless of the specific density estimation method used, a thorough understanding of the vocal behavior of the study species, particularly its vocalization rate, is required to estimate absolute density or abundance from such arrays.

ACKNOWLEDGMENTS

The data were collected for the NEAREST project, which was carried out on behalf of the EU Specific Programme "Integrating and Strengthening the European Research Area," Sub-Priority 1.1.6.3, "Global Change and Ecosystems," Contract No. 037110. We thank the German Instrument Pool for Amphibian Seismology (DEPAS), hosted by the Alfred Wegener Institute Bremerhaven, for providing the ocean bottom seismometers. The data analysis was conducted as part of the Ph.D. thesis by D.H. The thesis was funded by the U.K. Defence Science and Technology Laboratory, Grant No. RD034-014166. Further funding has been provided to D.H., L.M., and L.T. to extend the analysis by the Office of Naval Research under the "Cheap DECAF" project Grant No. N000141110615.

[1]P. Bromirski at Scripps Institution of Oceanography has also investigated tracking of fin and blue whales using three-component seismometers.

Aki, K., and Richards, P. (**1980**). *Quantitative Seismology, Theory and Methods* (Freeman and Company, San Francisco), Vol. 1, 557 pp.

Barlow, J., and Taylor, B. (**2005**). "Estimates of sperm whale abundance in the northeastern temperate Pacific from a combined acoustic and visual survey," Marine Mammal Sci. **21**(3), 429–445.

Buckingham, M. J. (**1998**). "Theory of compressional and shear waves in fluidlike marine sediments," J. Acoust. Soc. Am. **103**(1), 288–299.

Buckland, S. T., Anderson, D. R., Burnham, K. P., Laake, J. L., Borchers, D. L., and Thomas, L. (**2001**). *Introduction to Distance Sampling* (Oxford University Press, Oxford, UK), 432 pp.

Buckland, S. T., Anderson, D. R., Burnham, K. P., Laake, J. L., Borchers, D., and Thomas, L. editors (**2004**). *Advanced Distance Sampling* (Oxford University Press, Oxford, UK), 416 pp.

Carrara G., Matias, L., Geissler, W., D'Oriano, F., Lagalante, M., Cianchini, G., Chierici, F., Cuffaro, M., Diaconov, A., Doormann, U., Favali, P., Feld, C., Gerber, H., Gossler, J., Hansen, M., Innocenzi, L., Labahn, E., Langner, W., LoBue, N., Riminucci, F., Romsdorf, M., Salocchi, A., Unglert, K., Veneruso, M., Wolter, R. J., and Zitellini, N. (**2008**). "NEAREST 2008 cruise preliminary report r/v Urania," http://nearest.bo.ismar.cnr.it/documentation/nearest-2008-preliminary-report (Last viewed July 11, 2012).

Castellote, M., Clark, C. W., and Lammers, M. O. (**2012**). "Fin whale (*Balaenoptera physalus*) population identity in the western Mediterranean Sea," Marine Mammal Sci. **28**(2), 325–344.

Charif, R. A., Clapham P. J., and Clark C. W. (**2001**). "Acoustic detections of singing humpback whales in deep waters off the British Isles," Marine Mammal Sci. **17**(4), 751–768.

Charif, R. A., and Clark, C. W. (**2009**). "Acoustic monitoring of large whales in deep waters north and west of the British Isles: 1996–2005, Preliminary report," Technical Report 08-07, Cornell University Lab of Ornithology Bioacoustics Research Program, Ithaca, NY, 40 pp.

Croll, D. A., Clark, C. W., Acevedo, A., Tershy, B. R., Flores, R. S., Gedamke, J., and Urban, R. J. (**2002**). "Only male fin whales sing loud songs," Nature **417**, 809.

Delarue, J., Todd, S. K., Van Parijs, S. M., and Di Iorio, L. (**2009**). "Geographic variation in Northwest Atlantic fin whale (*Balaenoptera physalus*) song: Implications for stock structure assessment," J. Acoust. Soc. Am. **125**(3), 1774–1782.

Doyle, H. (**1995**). *Seismology* (Wiley and Sons, Chichester, UK), Chap. 14, pp. 123–137.

Dunn, R. A., and Hernandez, O. (**2009**). "Tracking blue whales in the eastern tropical Pacific with an ocean-bottom seismometer and hydrophone array," J. Acoust. Soc. Am. **126**(3), 1084–1094.

Frank, S. D., and Ferris, A. N. (**2011**). "Analysis and localization of blue whale vocalizations in the Solomon Sea using waveform amplitude data," J. Acoust. Soc. Am. **130**(2), 731–736.

Frohlich, C., and Pulliam, J. (**1999**). "Single-station location of seismic events: A review plea for more research," Phys. Earth Planet. Inter. **113**, 277–291.

Gillespie, D., Berggren, P., Brown, S., Kuklik, I., Lacey, C., Lewis, T., Matthews, J., McLanaghan, R., Moscrop, A., and Tregenza, N. (**2005**). "Relative abundance of harbour porpoises (*Phocoena phocoena*) from acoustic and visual surveys of the Baltic Sea and adjacent waters during 2001 and 2002," J. Cetacean Res. Manage. **7**(1), 51–57.

Goldbogen, J. A., Calambokidis, J., Friedlaender. A. S., Francis, J., DeRuiter, S. L., Stimpert, A. K., Falcone, E., and Southall, B. (**2013**). "Underwater acrobatics by the world's largest predator: 360° rolling manoeuvres by lunge-feeding blue whales," Biol. Lett. **9**(1), doi:10.1098/rsbl.2012.0986.

Incorporated Research Institutions for Seismology (**2011**), Washington, DC, http://www.iris.edu/manuals/rdseed.htm (Last viewed January 25, 2012).

International Whaling Commission (**2010**), http://iwcoffice.org/conservation/estimate.htm (Last viewed June 30, 2012).

Janik, V. (**2009**). "Whale song," Curr. Biol. **19**(3), 109–111.

Kerosky, S. M., Širović, A., Roche, L. K., Baumann-Pickering, S., Wiggins, S. M., and Hildebrand, J. A. (**2012**). "Bryde's whale seasonal range expansion and increasing presence in the Southern California Bight from 2000 to 2010," Deep-Sea Res., Part I **65**, 125–132.

Lurton, X. (**2002**). *An Introduction to Underwater Acoustics: Principles and Applications* (Praxis, Chichester, UK), 347 pp.

Marques, T. A., Munger, L., Thomas, L., Wiggins, S. and Hildebrand, J. A. (**2011**). "Estimating North Pacific right whale (*Eubalaena japonica*) density using passive acoustic cue counting," Endanger. Species Res. **13**, 163–172.

Marques, T. A., Thomas, L., Fancy, S. G., and Buckland, S. T. (**2007**). "Improving estimates of bird density using multiple covariate distance sampling," Auk **124**(4), 1229–1243.

Marques, T. A., Thomas, L., Martin, S. W., Mellinger, D. K., Jarvis, S., Morrissey, R. P., Ciminello, C.-A., and DiMarzio, N. (**2012**). "Spatially explicit capture recapture methods to estimate minke whale abundance from data collected at bottom mounted hydrophones," J. Ornithol. **152** (Suppl. 2), 445–455.

Marques, T. A., Thomas, L., Martin, S. W., Mellinger, D. K., Ward, J., Moretti, D., Harris. D., and Tyack, P. (**2013**). "Estimating animal population density using passive acoustics," Biol. Rev. **88**(2), 287–309.

Marques, T. A., Thomas, L., Ward, J., DiMarzio, N., and Tyack, P. L. (**2009**). "Estimating cetacean population density using fixed passive acoustic sensors: An example with Blainville's beaked whales," J. Acoust. Soc. Am. **125**, 1982–1994.

Martin, S. W., Marques, T. A., Thomas, L., Morrissey, R. P., Jarvis, S., DiMarzio, N., Moretti, D., and Mellinger, D. K. (**2013**). "Estimating minke whale (*Balaenoptera acutorostrata*) boing sound density using passive acoustic sensors," Marine Mammal Sci. **29**(1), 142–158.

Mathworks (**2012**). The Mathworks Inc., Cambridge, UK, http://www.mathworks.co.uk (Last viewed January 25, 2012).

McDonald, M. A. (**2006**). "An acoustic survey of baleen whales off Great Barrier Island, New Zealand," N.Z.J. Mar. Freshwater Res. **40**, 519–529.

McDonald, M. A., and Fox, C. G. (**1999**). "Passive acoustic methods applied to fin whale population density estimation," J. Acoust. Soc. Am. **105**, 2643–2651.

McDonald, M. A., Hildebrand, J. A., and Webb, S. C. (**1995**). "Blue and fin whales observed on a seafloor array in the Northeast Pacific," J. Acoust. Soc. Am. **98**(2), 712–721.

Moore, S. E., Howe, B. M., Stafford, K. M., and Boyd, M. L. (**2008**). "Including whale call detection in standard ocean measurements: Application of acoustic seagliders," Mar. Technol. Soc. J. **41**(4), 53–57.

Moretti, D., Marques, T., Thomas, L., DiMarzio, N., Dilley, A., Morrissey, R., McCarthy, E., Ward, J., and Jarvis, S. (**2010**). "A dive counting density estimation method for Blainville's beaked whale (*Mesoplodon densirostris*) using a bottom-mounted hydrophone field as applied to a Mid-Frequency Active (MFA) sonar operation," Appl. Acoust. **71**, 1036–1042.

NEAREST (**2012**). "Integrated Observations from Near Shore Sources of Tsunamis: Towards an Early Warning System," http://nearest.bo.ismar.cnr.it (Last viewed June 30, 2012).

Nieukirk, S. L., Mellinger, D. K., Moore, S. E., Klinck, K., Dziak, R. P., and Goslin, J. (**2012**). "Sounds from airguns and fin whales recorded in the mid-Atlantic Ocean, 1999–2009," J. Acoust. Soc. Am. **131**(2), 1102–1112.

Nieukirk, S. L., Stafford, K. M., Mellinger, D. K., Dziak, R. P., and Fox, C. G. (**2004**). "Low-frequency whale and seismic airgun sounds recorded in the mid-Atlantic Ocean," J. Acoust. Soc. Am. **115**(4), 1832–1843.

Notarbartolo di Sciara, G., Zanardelli, M., Jahoda, M., Panigada, S., and Airoldi, S. (**2003**). "The fin whale *Balaenoptera physalus* (L. 1758) in the Mediterranean Sea," Mamm. Rev. **33**, 105–150.

Ottemöller, L., Voss, P., and Havskov, J. (**2011**). "SEISAN: Earthquake analysis software for Windows, Solaris, Linux and Mac OSX."

Panigada, S., Pesante, G., Zanardelli, M., and Oehen, S. (**2003**). "Day and night-time behaviour of fin whales in the western Ligurian Sea," in *Proceedings of the Conference Oceans 2003*, September 22–26, 2003, San Diego, CA, pp. 466–471.

Rebull, O. G., Cusí J. D., Fernández M. R., and Muset J. G. (**2006**). "Tracking fin whale calls offshore the Galicia Margin, north east Atlantic ocean," J. Acoust. Soc. Am. **120**(4), 2077–2085.

Reilly, S. B., Bannister, J. L., Best, P. B., Brown, M., Brownell, R. L., Jr., Butterworth, D. S., Clapham, P. J., Cooke, J., Donovan, G. P., Urbán, J., and Zerbini, A. N. (**2008**). "*Balaenoptera physalus*," in: IUCN 2012. IUCN Red List of Threatened Species. Version 2012.2, http://www.iucnredlist.org (Downloaded February 19, 2013).

Roberts, R. G., Christoffersson, A., and Cassidy, F. (**1989**). "Real time events detection, phase identification and source location estimation using single station component seismic data and a small PC," Geophys. J. **97**, 471–480.

Shipboard Scientific Party (1972). "Sites 135," in Initial Reports of the Deep Sea Drilling Project (U.S. Government Printing Office, Washington, DC), Vol. 14, pp. 15–48.

Širović, A., Hildebrand, J. A., and Wiggins, S. M. (**2007**). "Blue and fin whale call source levels and propagation range in the Southern Ocean," J. Acoust. Soc. Am. **122**(2), 1208–1215.

Somoza, L., Anahnah, F., Bohoyo, F., González, J., Hernández, J., Iliev, I., León, R., Llave, E., Maduro, C., Martínez, S., Pérez, L. F., and Vázquez, T. (**2007**). "Informe científico-técnico, N/O L'ATALANTE," ("Scientific and technical report, R/V L'Atalante"), August 23 to September 9, 2007, project report, http://tierra.rediris.es/moundforce/Moundforce_informe_final.pdf (Last viewed February 25, 2013).

Soule, D. C., and Wilcock, J. S. (**2013**). "Fin whale tracks recorded by a seismic network on the Juan de Fuca Ridge, Northeast Pacific Ocean," J. Acoust. Soc. Am. **133**(3), 1751–1761.

Southall, B., Calambokidis, J., Tyack, P., Moretti, D., Hildebrand, J., Kyburg, C., Carlson, R., Friedlaender, A., Falcone E., Schorr, G., Douglas, A., DeRuiter, S., Goldbogen, J., and Barlow, J. (**2011**). "Biological and behavioral response studies of marine mammals in Southern California, 2010 (SOCAL-10)," Project Report, http://sea-inc.net/assets/pdf/SOCAL10_final_report.pdf (Last viewed July 11, 2012).

Stafford, K. M., Citta, J. J., Moore, S. E., Daher, M. A., and George, J. E. (**2009**). "Environmental correlates of blue and fin whale call detections in the North Pacific Ocean from 1997 to 2002," Mar. Ecol. Prog. Ser. **395**, 37–53.

Stafford, K. M., Mellinger, D. K., Moore, S. E., and Fox, C. G. (**2007**). "Seasonal variability and detection range modeling of baleen whale calls in the Gulf of Alaska, 1999–2002," J. Acoust. Soc. Am. **122**(6), 3378–3390.

Stafford, K. M., Nieukirk, S. L., and Fox, C. G. (**1999**). "An acoustic link between blue whales in the eastern tropical Pacific and the northeast Pacific," Marine Mammal Sci. **15**(4), 1258–1268.

Thomas, L., Buckland, S. T., Rexstad, E. A., Laake, J. L., Strindberg, S., Hedley, S. L., Bishop, J. R. B., Marques, T. A., and Burnham, K. P. (**2010**). "Distance software: Design and analysis of distance sampling surveys for estimating population size," J. Appl. Ecol. **47**, 5–14.

Thompson, P. O., Findley, L. T., and Vidal, O. (**1992**). "20-Hz pulses and other vocalizations of fin whales, Balaenoptera physalus, in the Gulf of California, Mexico," J. Acoust. Soc. Am. **92**, 3051–3057.

U.S. National Ocean Bottom Seismography Instrument Pool (OBSIP) (**2010**). accessed 17 May 2012, <http://www.obsip.org>.

Ward, J. A., Thomas, L., Jarvis, S., Baggenstoss, P., DiMarzio, N., Moretti, D., Morrissey, R. Marques, T. A., Dunn, C., Claridge, D., Hartvig E., and Tyack, P. (**2012**). "Passive acoustic density estimation of sperm whales in the Tongue of the Ocean, Bahamas," Marine Mammal Sci. **28**(4), E444–E455.

Watkins, W. A., Tyack, P., Moore, K. E., and Bird, J. E. (**1987**). "The 20-Hz signals of finback whales (*Balaenoptera physalus*)," J. Acoust. Soc. Am. **82**, 1901–1912.

Wiggins, S. M. (**2003**). "Autonomous acoustic recording package (ARPs) for long-term monitoring of whale sounds," Mar. Technol. Soc. J. **37**, 13–22.

Wilcock, W. S. D. (**2012**). "Tracking fin whales in the northeast Pacific Ocean with a seafloor seismic network," J. Acoust. Soc. Am. **132**(4), 2408–2419.

Wilcock, W. S. D., and Thomson, R. E. (**2010**). "Investigating the relationship between fin and blue whale locations, zooplankton concentrations and hydrothermal venting on the Juan de Fuca Ridge," ONR Project Report 2010, http://www.onr.navy.mil/reports/FY10/mbwilcoc.pdf (Last viewed July 11, 2012).